Canadian Science Publishing | Canadian Journal of Chemistry

Computational investigation of the effect of OH on the hydrogen evolution reaction by Nickel-bis(dithiolene) and Nickel-bis(diselenolene) complexes

Journal:	*Canadian Journal of Chemistry*
Manuscript ID	cjc-2020-0318.R1
Manuscript Type:	Article
Date Submitted by the Author:	25-Sep-2020
Complete List of Authors:	zhang, wenyuan; Brandon University, Lee, Changmin; Brandon University Bushnell, Eric; Brandon University, Chemistry
Is the invited manuscript for consideration in a Special Issue? :	Not applicable (regular submission)
Keyword:	density functional theory, Nickel-bis(dithiolene), Nickel-bis(diselenolene), Hydroxyl radical, Reactive Oxygen Species

Computational investigation of the reaction of Nickel-bis(dithiolene) and Nickel-bis(diselenolene) complexes with OH

*Wenyuan Zhang, Changmin Lee, and Eric A. C. Bushnell**

Department of Chemistry, Brandon University, 270-18th Street, Brandon, Manitoba R7A 6A9, Canada

AUTHOR EMAIL ADDRESS: bushnelle@brandonu.ca

RECEIVED DATE: to be inserted after the manuscript is accepted

TITLE RUNNING HEAD:

.

* Author to whom correspondence should be addressed. Email: bushnelle@brandonu.ca

Abstract

In the present study the reactivity of OH with $Ni(X_2C_2H_2)_2$ and $Ni(X_2C_2H_2)_2^-$ (where X = S or Se) was investigated. From the thermodynamics, it found that the OH radical attacks a backbone C-atom of the $Ni(S_2C_2H_2)_2$ complex. For the $Ni(Se_2C_2H_2)_2$ complex, the OH is predicted to target the ligating chalcogen atom. The significance of this is that with the attack of OH to a backbone C-atom, the thermodynamic cost to lose a proton or hydrogen atom ranges from exergonic to marginally endergonic depending on the oxidation state of the complex. Notably, such a process results in a rearrangement of the complex, likely leading to deactivation of the catalyst. Where OH has attacked a ligating chalcogenide atom, the thermodynamic cost to lose a proton or hydrogen is endergonic regardless of oxidation state of the complex.

Where OH attacks a coordinating chalcogenide atom, the thermodynamics for the addition of a proton was considered. At the present level of theory, it was found that for the dithiolene and diselenolene monoanionic complexes, the addition of a proton is marginally endergonic. However, following protonation, the loss of water is significantly exergonic and results in the regeneration of the neutral non-oxidized Ni-complex. Given the greater tendency for OH to attack Se versus S it may be speculated that the use of diselenolene ligands may offer a means to protect the Ni-complex from damaging OH radicals due to the thermodynamic tendency for OH to attack Se atom of the diselenolene complexes not seen in the dithiolene complexes.

Keywords: Nickel-bis(dithiolene), Nickel-bis(diselenolene), Density Functional Theory, Reactive Oxygen Species, Hydroxyl radical.

Introduction

Modern science requires finding new, eco-friendly alternative energy sources due to the threat of climate change.[1-4] Among the renewable energy sources, the most significant and most exploitable option available to humankind is solar energy with a potential of 60 terawatts of usable energy.[5-8] However, for us to depend on solar energy as an alternative energy source, we must be able to store it for later use during cloudy days and nights. One approach to storing solar energy is in the form of converting solar energy to chemical energy. For instance, the photocatalytic-production of molecular hydrogen gas (H_2(g)) via transition metal catalysts.[9] In comparison to other methods of hydrogen production, such as the electrolysis of coals to produce molecular hydrogen from water,[10-13] the use of solar energy to produce H_2(g) is environmentally friendly.

Recent work into the generation of hydrogen gas involves the use of transition metal dithiolene complexes.[14] In the work of Das et al.,[15] Ni-bis(dithiolene) complexes and analogs were investigated for their ability to reduce H^+ to H_2. The complexes investigated were $Ni(S_2(bdt))_2$, $Ni(SNH(bdt))_2$, $Ni(SO(bdt))_2$, and $Ni((NH)_2(bdt))_2$.[15] From the experimental evidence, it was concluded that the catalysts formed H_2(g) with high activity and exhibited notable durability.[15]

Thus, hydrogen production via dithiolene-metal complexes seems promising, but there are limitations to using these catalysts for the production of H_2. Specifically, the presence of impurities such as Cu(II) and other reactive species in homogeneous solution cause the catalysts to have poor durability.[9] It has been proposed that the poor durability comes from the high reactiveness of the dithiolene ligands with metal ions like Cu^{2+}, Fe^{3+}, and from reactive oxygen species in the solution.[9] Notably, free Cu^{2+} and Fe^{3+} ions produce radical oxygen species (ROS) in water.[16] ROS, such as superoxide anion (O_2^-), hydrogen peroxide (H_2O_2), and hydroxyl radicals ($OH^\bullet$) have the potential to inhibit catalytic activities when bound onto a catalyst.[17-18] For instance, ROSs have been shown to inactivate enzymatic activity of bacterial enzymes containing Fe-S clusters, such as aconitase.[17] In addition, to free metal ions, sunlight can also produce ROS as a result of ionizing radiation.[17] Notably, the superoxide anion and hydrogen peroxide are able to generate the very

reactive oxidant OH radical. OH radicals, despite their short life span of nanoseconds, are capable of dealing with considerable oxidative damage.

Unlike metal-dithiolene complexes, which have been investigated thoroughly, diselenolene-containing complexes have not been investigated intensively.[19] Recent work has revealed that dithiolene and diselenolene complexes are very similar in their geometrical and chemical properties.[20-22] However, despite the similarities between the two analogous complexes, diselenolene complexes are found to have a smaller HOMO-LUMO energy gap, suggesting higher reactivity of the molecule to electron transfer. A recent computational study[23] has compared the thermodynamics for H_2 production between Ni-bis(dithiolene) and -bis(diselenolene) complexes. From the work, it was predicted that in a dilute aqueous environment $Ni(Se_2C_2(NH_2)_2)_2$ and $Ni(Se_2C_2(CN)_2)_2$ are able to catalyze the formation of $H_2(g)$ with overall reaction Gibbs reaction energies of 8.7 kJ mol^{-1} and 8.4 kJ mol^{-1} (relative to the SHE), respectively. In another computational study,[24] the $Ni(SNHC_2(CN)_2)_2$ and $Ni(SeNHC_2(CN)_2)_2$ complexes were investigated using density functional theory to determine the thermodynamics associated with the electrocatalytic formation of $H_2(g)$. From the work the two complexes are indeed able to catalyze the production of H_2 gas under mildly reducing conditions relative to the SHE.[24] Notably, the thermodynamics for H_2 production are better for $Ni(SeNHC_2(CN)_2)_2$ than the analogous $Ni(SNHC_2(CN)_2)_2$ complex. It is noted that $Ni(SNHC_2(CN)_2)_2$ has been experimentally found to catalyze the formation of H_2 in aqueous solution.[24] Experimentally diselenolene complexes show significant improvement in durability under the prolonged reductive acidic situation, and recently, changing S atom to Se atom showed an improvement in the hydrogen evolution reaction (HER).[25]

Given the likely presence of OH radicals in a solution for the conversion of solar energy to chemical energy, the reactivity between the hydroxyl radical and $Ni(S_2C_2H_2)_2$was investigated using density functional theory (DFT). In addition, the chemistry of OH with $Ni(Se_2C_2H_2)_2$ was studied.

Methods

Optimized geometries, harmonic frequencies, and single-point energies of all compounds discussed herein were obtained with the Gaussian 09 computing suite.[26] The M06/def2-SVP level of theory was used for all geometry optimizations and the calculation of harmonic frequencies. The optimized geometries of all molecules investigated are given in the Supporting Information. Single point energies were obtained at the IEFPCM-M06/aug-cc-pVTZ//M06/def2-SVP level of theory and corrected to Gibbs energies by adding the Gibbs corrections obtained from the harmonic frequencies calculations at the M06/def2-SVP level of theory.[27-38] The M06 functional was chosen due to past work, which found that reduction potentials of several diselenolene complexes were in good agreement with those calculated at the CCSD level of theory.[27-28, 39-42] The M06 functional is a meta-hybrid GGA functional for general-purpose applications and is appropriate for use in transition metal chemistry.[27-28, 39] The IEFPCM approach was used to model the presence of solvent on the reaction with water chosen as the solvent.[30-33, 36, 43] In the calculation process, we tried to find transition structures for the attack of OH to the Ni, chalcogen atom, or backbone C atom. Specifically, we ran rigid scans where OH was moved closer to the complexes in 0.02 Å increments. However, the results for all scans at the present level of theory showed that no barriers in the electronic PES existed.

The reactions investigated herein involve a series of electron-transfer and proton-transfer steps. To calculate the Gibbs reaction energies ($\Delta_r G_s°$) for the proton transfer steps in a dilute aqueous environment, a chemical potential of -1124.2 kJ mol^{-1} was used for a proton.[44] To calculate the Gibbs reaction energies ($\Delta_r G_s°$) at 298 K for the electron-transfer steps, the chemical potential of -418.5 kJ mol^{-1} for the electron was used.[44] Such a value allows the Gibbs reaction energies for the electron-transfer steps to be made relative to the standard hydrogen electrode (SHE) Using $E° = -\Delta_r G_s°/F$ the relative Gibbs energies for the electron-transfer steps were converted to reduction potentials.

Using the density functions calculated at the IEFPCM-M06/aug-cc-pVTZ//M06/def2-SVP level of theory the Mutiwfn program was used to carry out the orbital analysis.[45]

Results and Discussion

In past studies of the $Ni(X_2C_2(CN)_2)_2$, $Ni(X_2C_2(NH_2)_2)_2$ and $Ni(XNHC_2(CN)_2)_2$ (where X = S or Se) complexes it was found that prior to the reduction of H^+ to form H_2 the complexes must undergo two one-electron reductions.[23-24] Therefore, for the complexes investigated herein, the reduction potentials of the ($Ni(X_2C_2H_2)_2/Ni(X_2C_2H_2)_2^{1-}$) and ($Ni(X_2C_2H_2)_2^{1-}/Ni(X_2C_2H_2)_2^{2-}$) (where X = S or Se) redox couples relative to the SHE were calculated. At the IEFPCM-M06/aug-cc-pVTZ//M06/def2-SVP level of theory, the reduction potentials for the ($Ni(S_2C_2H_2)_2/Ni(S_2C_2H_2)_2^{1-}$) and ($Ni(S_2C_2H_2)_2^{1-}/Ni(S_2C_2H_2)_2^{2-}$) redox couples were calculated to be 0.35 V, and -0.08 V, respectively. Regarding the $Ni(Se_2C_2H_2)_2/Ni(Se_2C_2H_2)_2^{1-}$) and ($Ni(Se_2C_2H_2)_2^{1-}/Ni(Se_2C_2H_2)_2^{2-}$) redox couples the values were calculated to be 0.34 V, and -0.08 V, respectively. It is noted that all reduction potentials were made relative to the SHE (see Methods section for details). Therefore, given the endergonicity of the second reduction relative to the SHE, the reaction of S0, S-1, Se0, and Se-1 with the OH radical was only considered herein.

The frontier molecular orbitals involved in the reaction were considered to predict the location where the hydroxyl radical attacks the $Ni(S_2C_2H_2)_2$ and $Ni(Se_2C_2H_2)_2$ complexes. The SOMO and HOMO of the reduced and neutral forms of Ni-bis(dithiolene) and -bis(diselenolene), and the SOMO of OH are shown in **Figure 1**.

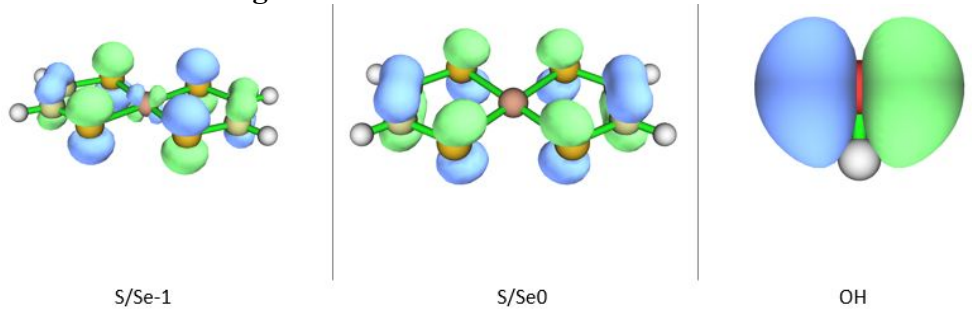

Figure 1 The SOMO and HOMO of the reduced (S/Se-1)and neutral (S/Se0) forms of Ni-

bis(dithiolene) and -bis(diselenolene) complexes and hydroxyl radical.

For a better understanding of the potential difference in the HOMO/SOMO contributions caused by the change in coordinating chalcogen atom, a Mulliken orbital composition analysis was done on the HOMO of S0, Se0, and the SOMO of S-1 and Se-1. From the analysis, it found that the nickel atom, sulfur atoms and carbon atoms contribute 6.8%, 51.2%, and 41.6% to the HOMO. For Se0, the HOMO is constructed by 6.4% nickel atom, and the contribution of sulfur atoms and carbon atoms are 58.0% and 35.0%, respectively. Regarding the SOMO of S-1, the nickel atom, the sulfur atoms, and backbone carbon atoms contribute 8.0%, 67.2%, and 20.5%, respectively. For Se-1, the respective values are 8.2%, 70.6%, and 21.0%. Therefore, it is expected that the hydroxyl radical has three possible binding sites to the $Ni(S_2C_2H_2)_2$ and $Ni(Se_2C_2H_2)_2$ complexes, the Ni-center, a coordinating chalcogen atom, and a ligand backbone C-atom

In the case of S0-Ni and S-1-Ni, the planar coordination geometry around the Ni-center has been lost due to the formation of a new coordination bond between the nickel and the OH. The attack of the OH to a sulfur atom results in the formation of S0-S, and S-1-S. With the attack of the OH to a backbone C-atom the products S0-C and S-1-C are formed. Regarding S0-S, S-1-S, S0-C, and S-1-C, the planar coordination geometry around the Ni-center is maintained, and the coordination geometry of the metal center is marginally affected by the attack of OH. However, regarding the attack on the C-atom, the ligand π-electron system is destroyed. Specifically, with the attack by OH, it was found that the S-atom vicinal to the OH group no longer contributes to the redox-active MO resulting in the loss of the fully delocalized redox-active MO over the entire Ni-complex for S0-C and S-1-C (**Figures S1 and S3**). In the case of S0-S and S-1-S, this was not the case, and we can see continued delocalization of the redox-active MO over the entire complexes (**Figures S2 and S4**). Thus, the chemistry of the complexes is expected to be negatively affected by the attack of the OH to the backbone carbon atom. For S0-C and S-1-C, changes in the ligand geometry are observed as a result of oxidation. Specifically, the S-C-C-S dihedral angle has

become 18.26°, and 34.14°, for S0-C, and S-1-C, respectively. While structural changes are observed for all OH products, no bond cleavages are observed in the complexes, which would immediately lead to the deactivation of the complexes.

For the $Ni(Se_2C_2H_2)_2$ complex, the optimization of the three possible products was done for both oxidation states. Regarding the attack of the OH to the Ni center, it was found that during the optimization, a Ni-OH coordination bond did not form. Rather, the OH group migrated to a coordinating Se-atom. A possible reason for this is because the valence electrons of selenium occupy larger space than sulfur and thus shield the nickel d-orbitals more effectively. Therefore, in the optimization of the diselenolene complexes, only two possible products were formed. Depending on the oxidation state of the complex, with the attack of the OH to a coordinating Se atom, the products Se0-Se, and Se-1-Se are formed. With the attack of the OH to a C-atom in the ligand backbone, Se0-C and Se-1-C are formed. Like that seen for the dithiolene complexes, the products formed to maintain a planar coordination geometry around the Ni-center. Moreover, like the dithiolene complexes with the formation of Se0-C, and Se-1-C, the ligand π-electron system is destroyed. Specifically, with the attack by OH, it was found that the Se-atom vicinal to the OH group no longer contributes to the redox-active MO resulting in the loss of the fully delocalized redox-active MO over the entire Ni-complex. In the case of the Se0-Se and Se-1-Se, this was not the case, and we see continued delocalization of the redox-active MO over the entire complexes. For all OH products, no bond cleavages are observed, which would immediately lead to the deactivation of the complexes. However, for Se0-C and Se-1-C, the Se-C-C-Se dihedral angles were calculated to be 17.66° and 20.19°, respectively. Thus, from the dihedral angles calculated, the diselenolene complexes appear to have a better ability to resist structural changes when hydroxyl radicals attack the backbone C-atoms.

The Gibbs energies for OH attack of the neutral and reduced Ni-complexes are given in **Figures 2** and **3**.

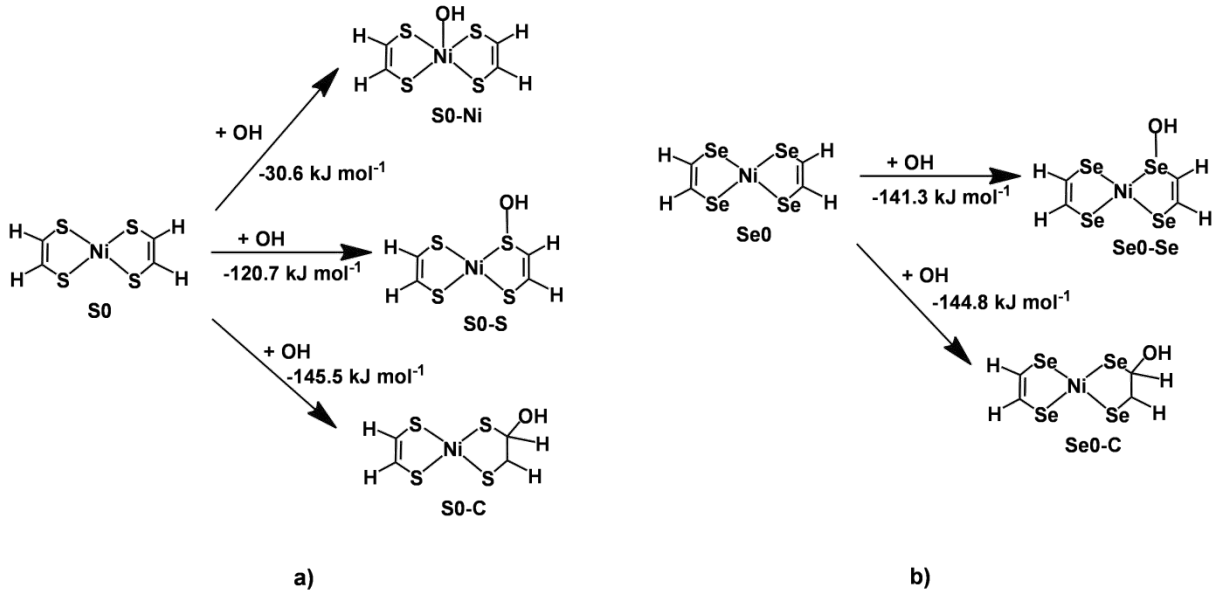

Figure 2 Gibbs reaction energies for the attack of OH to a) S0 and b) S0.

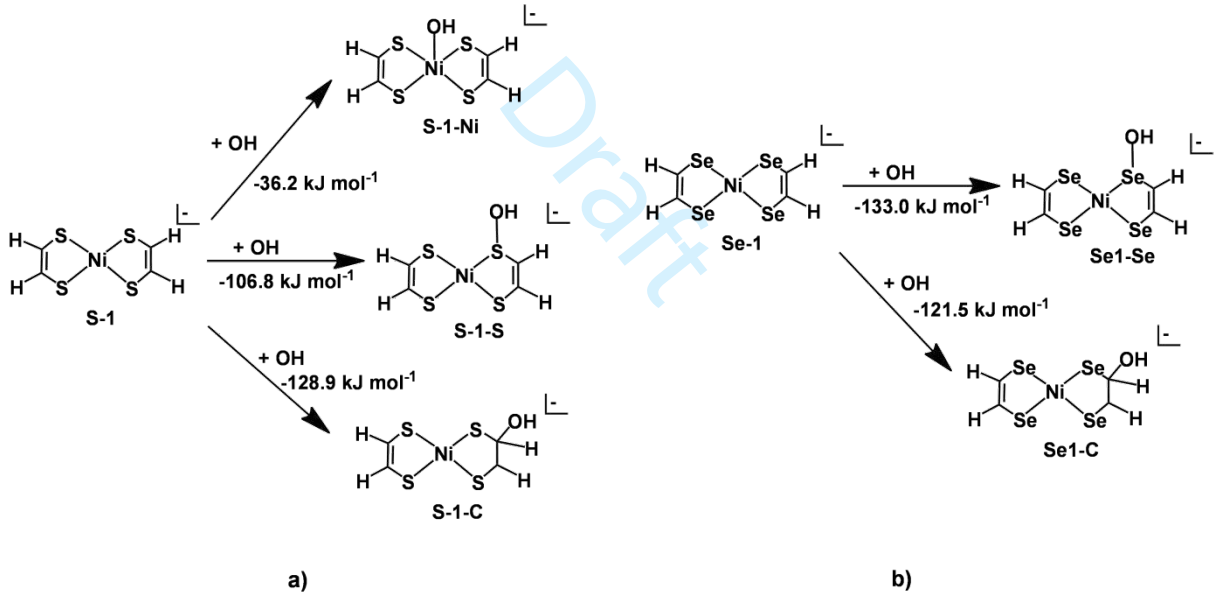

Figure 3 Gibbs reaction energies for the attack of OH to a) S-1 and b) Se-1.

From **Figure 2,** the attack of OH to the Ni-atom of the S0 complex occurs with a Gibbs reaction energy ($\Delta_rG°$) of -30.6 kJ mol^{-1}. With the attack of the OH to the S-atom, $\Delta_rG°$ is calculated to be -120.7kJ mol^{-1}. The most exergonic process is the attack of OH to a backbone carbon atom with a calculated Gibbs reaction energy of -145.5 kJ mol^{-1}, resulting in the formation of S0-C. For Se0,

the Gibbs reaction energy of the hydroxyl radical binding to the selenium-atom is -144.3 kJ mol^{-1}, whereas the Gibbs reaction energy for the binding to a carbon atom is -144.8kJ mol^{-1}.

For the reduced S-1 and Se-1 species, the attack of OH remains exergonic (**Figure 3**). However, from the calculated Gibbs reaction energies, the attack of OH to the reduced complexes is, on average, 26 kJ mol^{-1} less exergonic. Regardless, it is expected that in the presence of OH radicals, the S0, Se0, S-1, and Se-1 will readily bind to the OH.

From the energies provided in **Figures 2** and **3**, the attack of OH to S0 and Se0 has the effect of reducing the oxidizing power of the Ni-complexes. As noted above, the reduction potentials for the ($Ni(S_2C_2H_2)_2/Ni(S_2C_2H_2)_2^{1-}$) and $Ni(Se_2C_2H_2)_2/Ni(Se_2C_2H_2)_2^{1-}$) were calculated to be 0.35 V, and 0.34 V, respectively. For the (S0-S/S-1-S) and (Se0-Se/Se-1-Se) redox couples, the calculated reduction potentials were 0.21 V and 0.25 V, respectively. For the case where the OH attacks the carbon atom, the (S0-C/S-1-C) and (Se0-C/Se-1-C) redox couples were calculated to have reduction potentials of 0.18 V and 0.10 V, respectively. However, regardless, it is possible that OH may readily attack the neutral complexes, and in the presence of a reducing agent, become quickly reduced relative to the SHE.

From the energies given in **Figures 2** and **3,** the presence of the selenium atoms confers greater reactivity of the OH to the chalcogen atom when compared to the S-atom. To estimate the relative amounts of species present, the Boltzmann probability distribution equation was used on the Gibbs reaction energies provided in **Figures 2** and **3**. Following the OH attack, the most likely distribution is the S0-C product is 100%. However, with the attack of OH to Se0, it is expected to exist as Se0-Se 45.2% and Se0-C 54.8%. If Se0 is reduced first, the proportion of Se-1-Se products expands to 99.0%, whereas the proportion of Se-1-C decreases to 1.0%. For the dithiolene complexes, the S-1-C ratio is still 100%. Thus, the substitution of selenium atoms for sulfur atoms significantly increased the proportion of free radicals bonding to the chalcogen atom.

To identify if a possible rearrangement of the Ni-complex is thermodynamically feasible. The possibility of losing a proton (H^+) or H-atom ($H^\bullet$) from the OH moiety was considered for all

oxidized complexes. Such rearrangement may lead to irreversible deactivation of the catalyst. The Gibbs reaction energies for the loss of H^+ or $H^\bullet$ are given in **Figures 4 - 7**. The first treatment is the removal of an H^+ from the OH group. This creates a negative charge for possible rearrangement. The second treatment is the removal of a hydrogen atom ($H^\bullet$) from the OH group via a proton-coupled electron transfer. In other words, the proton may originate from the OH group, whereas the electron may leave from the dithiolene complex or OH group. With H^+ or $H^\bullet$ loss r a sulfoxide or selenoxide functional group is formed (**Figures 4** and **5**). In the structure comparison, the products formed after loss of H^+ or $H^\bullet$ maintain their coordination to the Ni-atom. For the case where OH attacked the sulfur atom (S0-S), the Gibbs reaction energy for the loss of an H^+ is 31.2 kJ mol^{-1}, whereas the loss of a hydrogen atom is twice as endergonic (**Figure 4**). For the same changes in the Se0-Se analog, the Gibbs reaction energies were 69.6 kJ mol^{-1} and 126.6 kJ mol^{-1}, respectively (**Figure 4**). For S-1-S and Se-1-Se, the loss of a proton is considerably endergonic with calculated Gibbs reaction energies of 79.3 kJ/mol and 111.9 kJ mol^{-1} (**Figure 5**), respectively. Regarding the loss of a hydrogen atom, the Gibbs reaction energies are 50.9 kJ mol^{-1} and 94.0 kJ mol^{-1}, respectively. Thus, for the complexes investigated, the loss of a proton or hydrogen atom is endergonic and is not expected to happen spontaneously from S0-S, S-1-S, Se0-Se, and Se-1-Se in a dilute aqueous environment relative to the SHE.

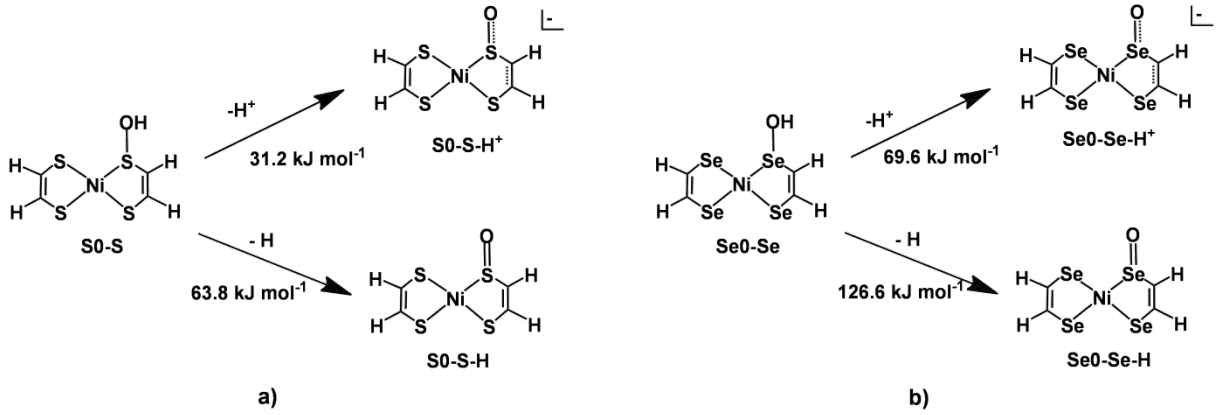

Figure 4 Gibbs reaction energies for the loss of H^+ and $H^\bullet$ from S0-S and Se0-Se.

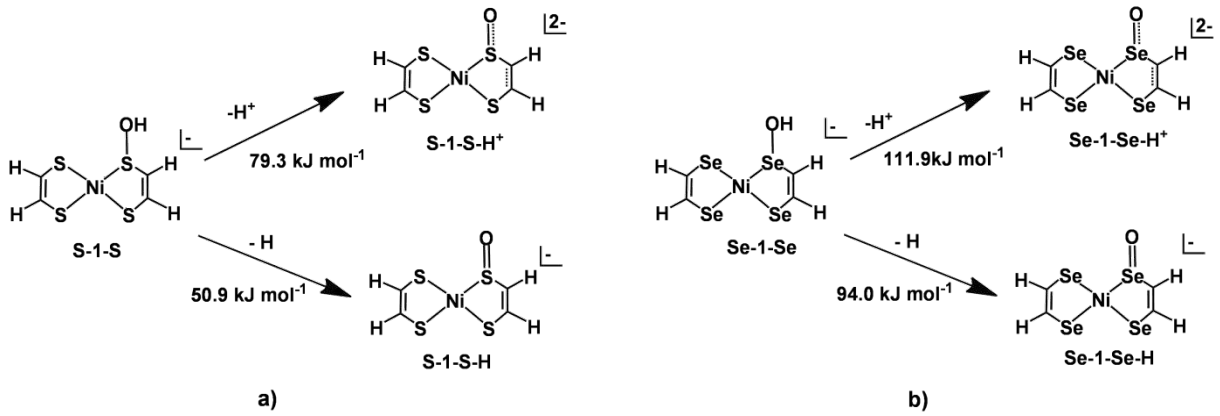

Figure 5 Gibbs reaction energies for the loss of H^+ and $H^\bullet$ from S-1-S and Se-1-Se.

Where OH has attacked a backbone carbon atom, considerable rearrangement in the complex occurs with the removal of an H^+ (**Figure 6)**. For S0-C, it was found that hydrogen from the carbon bound to the OH migrates to the adjacent carbon atom (**Figure 6**). This rearrangement was also observed when an H^+ is removed from Se0-C. As seen in **Figure 6,** this rearrangement is a considerably exergonic process that releases 117 kJ mol^{-1} and 119.4 kJ mol^{-1} for S0-C, and Se0-C, respectively. For the reduced complexes (i.e., S-1-C and Se-1-C), the loss of proton results in the formation of an epoxide functional group (**Figure 7**).

With the removal of a hydrogen atom, considerable structural changes to the molecules is observed. For S0-C, when $H^\bullet$ is removed, hydrogen migrates from the carbon bound to the OH to the adjacent S-atom (**Figure 6**). For the S0-C-H complex, with the transfer of the hydrogen atom, a considerable lengthening (Δ_r = 0.084Å) in the C-S bond is observed, indicating a weakening in the S-Ni coordination. A similar observation was seen for Se0-C-H, where lengthening of 0.082Å was observed in the C-Se bond. In terms of Gibbs energy, this change is a marginally endergonic reaction requiring 11 kJ mol^{-1} and 6.6 kJ mol^{-1}, for S0-C and Se0-C respectively (**Figure 6**) With the removal of a hydrogen atom from S-1-C and Se-1-C the complexes rearrange to form an epoxide which occurs with Gibbs reaction energies of 50.9 kJ mol^{-1} and 24.5 kJ mol^{-1}, respectively (**Figure 7**).

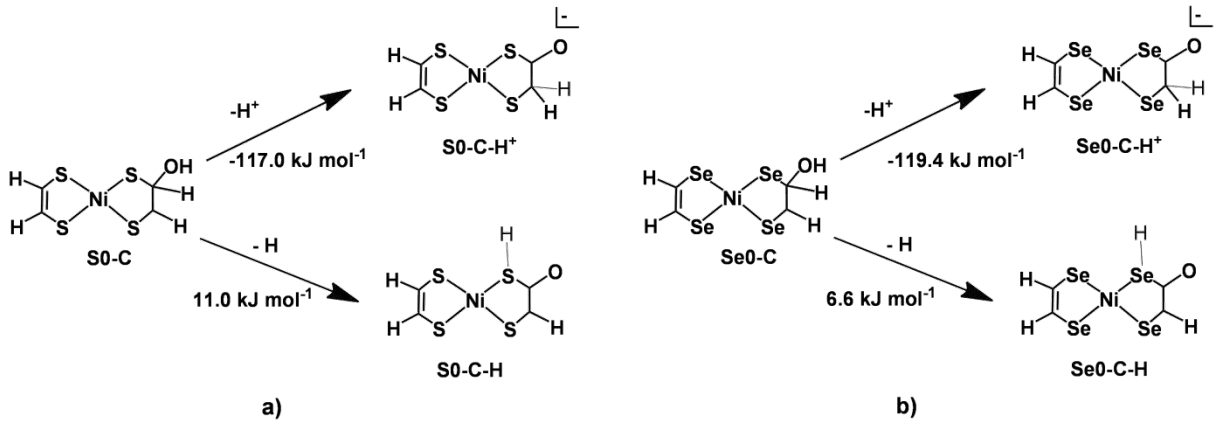

Figure 6 The Gibbs reaction energies for the loss of H^+ and $H^\bullet$ from S0-C and Se0-C.

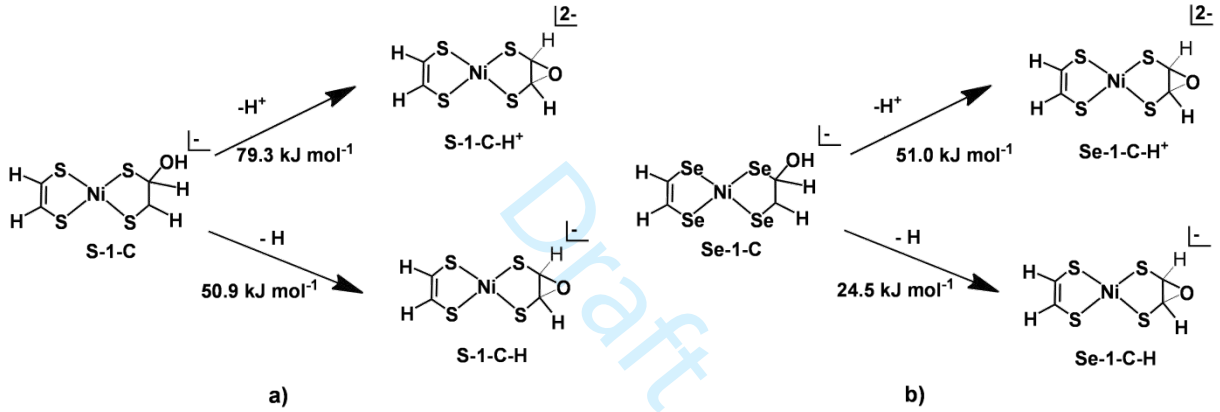

Figure 7 The Gibbs reaction energies for the loss of H^+ and $H^\bullet$ from S-1-C and Se-1-C.

In the case of S0-Ni and S-1-Ni, the energies for loss of H^+ and $H^\bullet$ are given in **Figure 8**. From the energies provided, the only process that is expected to happen spontaneously in a dilute aqueous environment is the loss of a proton from S0-Ni to form S0-Ni-H+. However, as shown in **Figure 8** to go from SX-Ni to SX-S (X=0 or -1) occurs with a low Gibbs activation energy. Therefore, it is expected that S0-Ni and S-1-Ni will quickly rearrange to form S0-S and S-1-S, respectively.

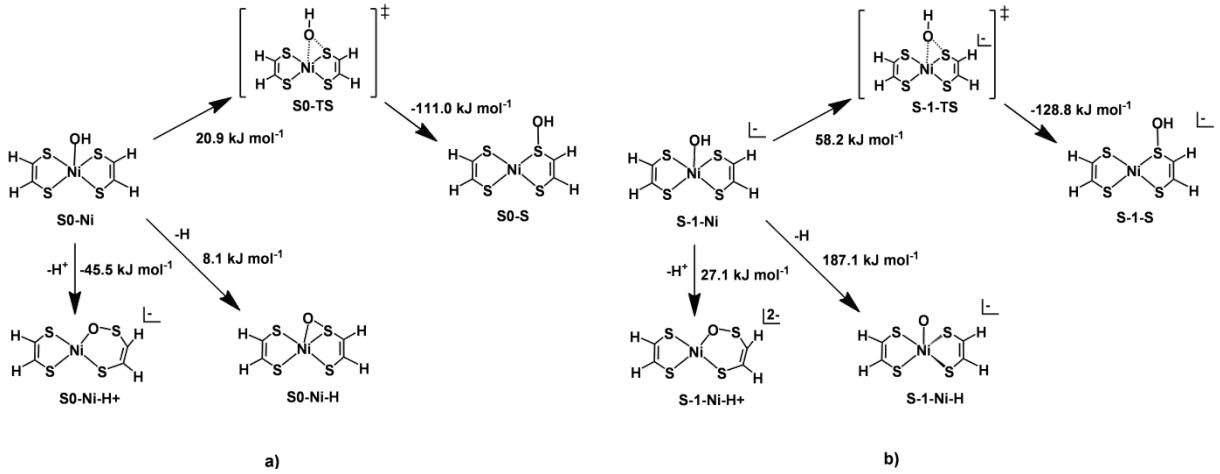

Figure 8 Gibbs reaction energies for the rearrangement between SX-Ni and SX-S (where X = 0 or -1) and for the loss of H+ and H• from SX-Ni.

As mentioned above, the two molecules, SX-C/SeX-C (where X = 0 or -1), are prone to rearrangement at neutral valence, where the rearrangement of S0-C-H+ and Se0-C-H+ can form a thermodynamically stable molecule. From the previous discussion, S0-C is the main product of OH radical attack, whereas, for the Se-containing catalysts, a large fraction of the Se0-Se complex is expected to form. However, with the formation of S0-C and Se0-C, the calculated reduction potentials suggest that in a dilute aqueous environment, the S-C and Se0-C will be reduced. From the values presented in **Figures 4 – 7,** if the complexes are reduced, it is unlikely that they will lose a proton or hydrogen atom to rearrange spontaneously under standard conditions.

According to the catalytic mechanism proposed by Zarkadouls et al. .[42], hydrogen gas is generated after two hydrogen ions (H^+) are added to different coordinating chalcogen atoms of the metal complex. Thus, we considered the Gibbs reaction energies for the addition of the proton to the oxidized and reduced complexes (**Figures 9 – 11**). For the resulting SX-S+H+ and SeX-Se+H+ complexes, we also considered the Gibbs reaction energies for further reduction to determine the energetic cost to regenerate the Ni-complex prior to OH attack. Also shown in **Figures 9 - 11** is the Gibbs energy cost to form water molecules and recycle the catalyst.

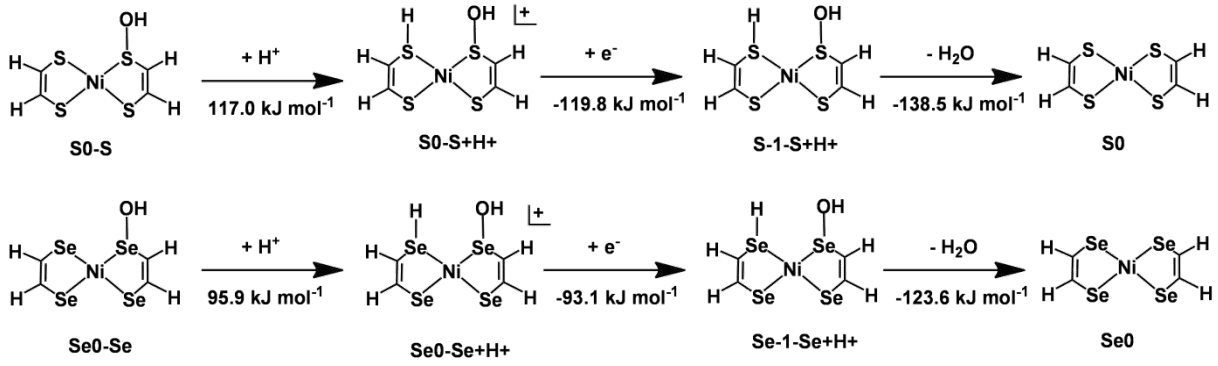

Figure 9 Gibbs reaction energies for the recovery of the S0 and Se0 catalysts from S0-S and Se0-Se, respectively.

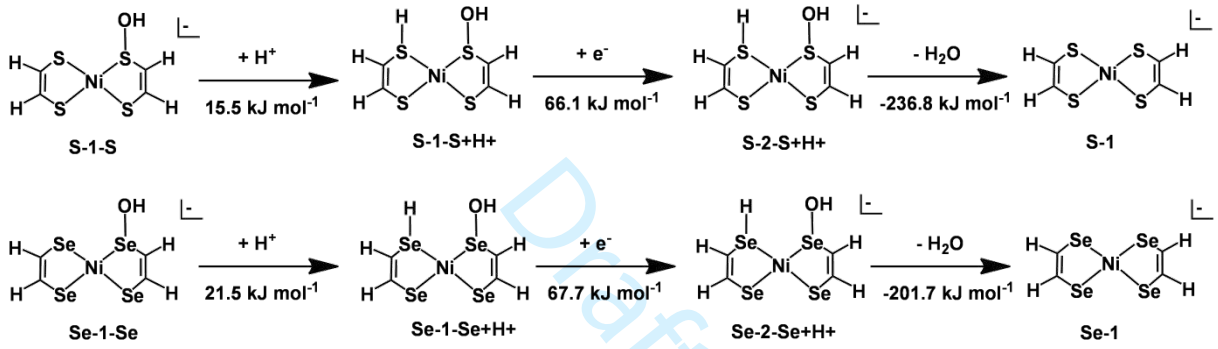

Figure 10 Gibbs reaction energies for the recovery of the S-1 and Se-1 catalysts from S-1-S and Se-1-Se, respectively.

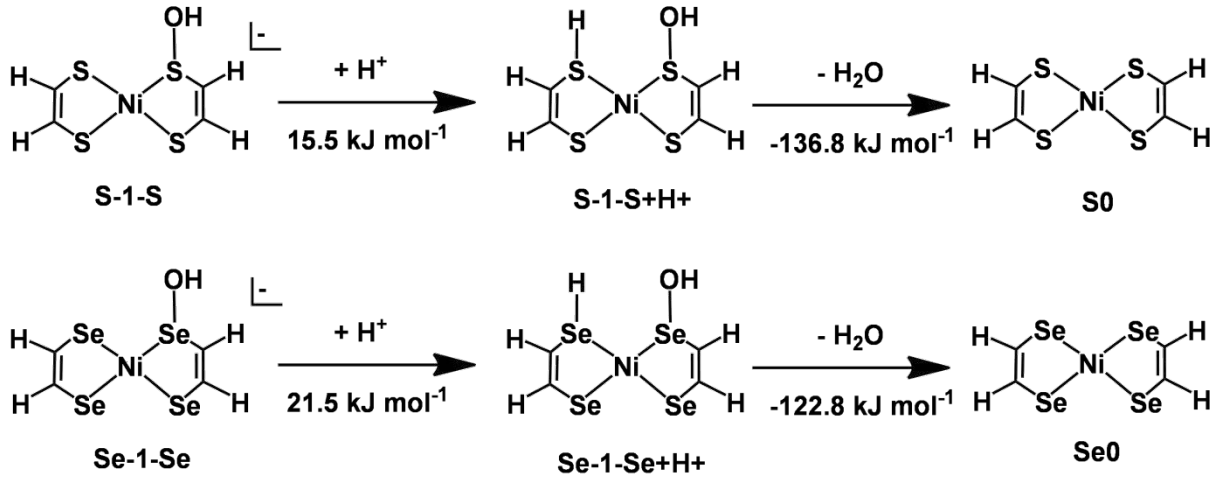

Figure 11 Gibbs reaction energies for the recovery of the S0 and Se0 catalysts from S-1-S and Se-1-Se, respectively.

From **Figures 9** and **10,** the Gibbs reaction energies to recover the catalyst is thermodynamically unlikely to happen under the two valence states. When the complexes are neutral, the addition of the proton to the S0-S and the Se0-Se complexes, is considerably endergonic, where $\Delta_r G°$ is found to be 117 kJ mol^{-1} and 95.9 kJ mol^{-1}, respectively. However, the addition of an electron following protonation is considerably exergonic (**Figure 9**). With the formation of S-1-S+H+ and Se-1-Se+H+, the loss of H_2O to regenerate the S0 and Se0 catalysts, respectively, is considerable exergonic (**Figure 9)**. In the case of S-1-S and Se-1-Se, protonation is only marginally endergonic; however, further reduction to form S-2-S+H+ and Se-2-Se+H+ is not thermodynamically favorable relative to the SHE (**Figure 10**) However, if S-2-S+H+ and Se-2-Se+H+ are formed, the loss of H_2O to reform S-1 and Se-1, respectively, is considerably exergonic. But an alternative reaction path exists, as shown in **Figure 11**. As seen in **Figure 11**, the thermodynamic cost to generate H_2O from S-1-S and Se-1-Se to form S0 and Se0, respectively, is thermodynamically feasible in a dilute aqueous environment. Importantly, while the recovery of S0 and Se0 from S-1-S and Se-1-Se, respectively, appears thermodynamically favorable, from the relative energies provided in **Figure 3,** only Se-1-Se is likely to exist in great concentrations in a dilute aqueous environment.

Conclusion

In the present investigation, the reactivity of the OH radical with Ni-bis(dithiolene) and Ni-bis(diselenolene) was studied. Regarding the neutral and monoanionic dithiolene complexes, the attack of OH to the C-atom is, on average, 23.3 kJ mol^{-1} more exergonic than the attack to a ligating chalcogen atom. However, in the case of the diselenolene complexes, the attack of OH to a backbone C-atom is, on average, only 4.0 kJ mol^{-1} more endergonic than attack to a ligating Se-atom. Thus, for the dithiolene complexes, the product formed is essentially the oxidized C-atom product for both the neutral and monoanionic complex, whereas, for the diselenolene complexes,

the oxidized C-atom product makes up only 55% and 5% for the oxidized neutral and monoanionic complexes, respectively.

In the case where the OH has attacked a ligating chalcogen atom, the thermodynamic cost to lose a proton or hydrogen ranges from +31.2 kJ mol^{-1} to +126.6 kJ mol^{-1} under standard conditions. However, with an attack of OH to a backbone C-atom, the thermodynamic cost to lose a proton or hydrogen atom ranges from -117.0 kJ mol^{-1} to +79.3 kJ mol^{-1} under standard conditions, depending on the oxidation state of the complex. Notably, the loss of proton or hydrogen atom from the OH moiety when bound to a backbone C-atom results in a rearrangement of the complex that likely leads to the deactivation of the catalyst. Therefore, the dithiolene complexes are expected to have a greater thermodynamic tendency to be deactivated, whereas the diselenolene complexes are less likely due to the greater formation of the oxidized chalcogen-atom product.

Given the greater tendency for OH to attack the ligating Se-atom versus the S-atom, the thermodynamic cost for the addition of a proton to the oxidized complexes was considered. It was found that for the dithiolene and diselenolene monoanionic complexes, the addition of a proton is marginally endergonic with Gibbs reaction energies of +15.5 kJ mol^{-1} and +21.5 kJ mol^{-1}, respectively. However, following protonation, the loss of water is significantly exergonic with Gibbs reaction energies of -136.8 kJ mol^{-1} and -122.8 kJ mol^{-1}, respectively. Notably, with the loss of water, the neutral non-oxidized Ni-complex is regenerated. Therefore, given the greater tendency for OH to attack Se versus S it may be speculated that the use of diselenolene ligands may offer a means to protect the Ni-complex from damaging OH radicals due to the thermodynamic tendency for OH to attack Se atom of the diselenolene complexes not seen in the dithiolene complexes.

Supporting information

Table S1 contains all XYZ coordinates of optimized structures. **Figure S1 –S4** show the SOMO and HOMO of S0-C/S0-S and S-1-C/S-1-S, respectively.

References

1. Esswein, A. J.; Nocera, D. G., Hydrogen Production by Molecular Photocatalysis. *Chem. Rev.* **2007,** *107* (10), 4022-4047.
2. Eckenhoff, W. T.; Eisenberg, R., Molecular systems for light driven hydrogen production. *Dalton Trans.* **2012,** *41* (42), 13004-13021.
3. Lewis, N. S.; Nocera, D. G., Powering the planet: Chemical challenges in solar energy utilization. *Proc. Natl. Acad. Sci. U.S.A.* **2006,** *103* (43), 15729-15735.
4. Cook, T. R.; Dogutan, D. K.; Reece, S. Y.; Surendranath, Y.; Teets, T. S.; Nocera, D. G., Solar Energy Supply and Storage for the Legacy and Nonlegacy Worlds. *Chem. Rev.* **2010,** *110* (11), 6474-6502.
5. Bard, A. J.; Fox, M. A., Artificial Photosynthesis: Solar Splitting of Water to Hydrogen and Oxygen. *Acc. Chem. Res.* **1995,** *28* (3), 141-145.
6. Eisenberg, R., Rethinking Water Splitting. *Science* **2009,** *324* (5923), 44-45.
7. Blanco, J.; Malato, S.; Fernández-Ibañez, P.; Alarcón, D.; Gernjak, W.; Maldonado, M. I., Review of feasible solar energy applications to water processes. *Renewable Sustainable Energy Rev.* **2009,** *13* (6), 1437-1445.
8. Zhang, Y.; Sivakumar, M.; Yang, S.; Enever, K.; Ramezanianpour, M., Application of solar energy in water treatment processes: A review. *Desalination* **2018,** *428*, 116-145.
9. Zarkadoulas, A.; Koutsouri, E.; Mitsopoulou, C. A., A perspective on solar energy conversion and water photosplitting by dithiolene complexes. *Coord. Chem. Rev.* **2012,** *256* (21), 2424-2434.
10. Hesenov, A.; Kınık, H.; Puli, G.; Gözmen, B.; Irmak, S.; Erbatur, O., Electrolysis of coal slurries to produce hydrogen gas: Relationship between CO2 and H2 formation. *Int. J. Hydrogen Energy* **2011,** *36* (9), 5361-5368.
11. Katakis, D., Mechanisms of Homogeneous Stoichiometric, Catalytic and Photocatalytic Dihydrogen Formation Using Thiocomplexes. *Pure Appl. Chem.* **1988,** *60*, 1285-1290.

12. Amouyal, E., Photochemical production of hydrogen and oxygen from water: A review and state of the art. *Sol. Energy Mater. Sol. Cells* **1995,** *38* (1), 249-276.

13. Steinfeld, A., Solar thermochemical production of hydrogen—a review. *Sol. Energy* **2005,** *78* (5), 603-615.

14. Zarkadoulas, A.; Koutsouri, E.; Semidalas, E.; Psycharis, V.; Raptopoulou, C. P.; Mitsopoulou, C. A., Photocatalytic hydrogen production with alkylated nickel bis-dithiolene complexes. *Polyhedron* **2018,** *152*, 138-146.

15. Das, A.; Han, Z.; Brennessel, W. W.; Holland, P. L.; Eisenberg, R., Nickel Complexes for Robust Light-Driven and Electrocatalytic Hydrogen Production from Water. *ACS Catal.* **2015,** *5* (3), 1397-1406.

16. Keshavarz, F.; Mazarei, E., From Kinetics of OH Reaction with Glutamic Acid to Oxidative Damage to Proteins. *J. Phys. Chem. A* **2019,** *123* (2), 429-442.

17. Darley-Usmar, V.; Halliwell, B., Blood radicals: reactive nitrogen species, reactive oxygen species, transition metal ions, and the vascular system. *Pharm. Res.* **1996,** *13* (5), 649-62.

18. Damgaard, D.; Bjørn, M. E.; Jensen, P. Ø.; Nielsen, C. H., Reactive oxygen species inhibit catalytic activity of peptidylarginine deiminase. *J. Enzyme Inhib. Med. Chem.* **2017,** *32* (1), 1203-1208.

19. Davison, A.; Shawl, E. T., The Preparation Of Bis(Trifluoromethyl)-1,2-Diselenetene And Some 1,2-Diselenolene Transition Metal Complexes. *Inorg. Chem.* **1970,** *9* (8), 1820-1825.

20. Bushnell, E. A. C., A Computational Investigation Into The Catalytic Activity Of A Diselenolene Sulfite Oxidase Biomimetic Complex. *Can. J. Chem.* **2016,** *94* (12), 1127-1132.

21. Bushnell, E. A. C.; Adams, M. R.; Boyd, R. J., A Computational Investigation into the Redox Chemistry of Mo- and W-tris(diselenolene) complexes. *Struct. Chem.* **2017,** *28*, 1173-1180.

22. Bushnell, E. A. C.; Boyd, R. J., Identifying similarities and differences between analogous bisdithiolene and bisdiselenolene complexes: A computational study. *Int. J. Quantum Chem.* **2016,** *116* (5), 369–376.

23. Boychuk, B. T. A.; Bushnell, E. A. C., A computational investigation into nickel-bis(diselenolene) complexes as potential catalysts for reduction of H+ to H2. *Can. J. Chem.* **2017,** *96* (1), 51-57.

24. Abad, K. P.; Bushnell, E. A. C., Computational Investigation into the Ni(SeNHC2(CN)2)2 and Ni(SNHC2(CN)2)2 Complexes as Potential Catalysts for Hydrogen Production. *J. Phys. Chem. A* **2019,** *123* (36), 7822-7827.

25. Downes, C. A.; Marinescu, S. C., Bioinspired Metal Selenolate Polymers with Tunable Mechanistic Pathways for Efficient H2 Evolution. *ACS Catal.* **2017,** *7* (1), 848-854.

26. Frisch, M. J.; Trucks, G. W.; Schlegel, H. B.; Scuseria, G. E.; Robb, M. A.; Cheeseman, J. R.; Scalmani, G.; Barone, V.; Mennucci, B.; Petersson, G. A.; Nakatsuji, H.; Caricato, M.; Li, X.; Hratchian, H. P.; Izmaylov, A. F.; Bloino, J.; Zheng, G.; Sonnenberg, J. L.; Hada, M.; Ehara, M.; Toyota, K.; Fukuda, R.; Hasegawa, J.; Ishida, M.; Nakajima, T.; Honda, Y.; Kitao, O.; Nakai, H.; Vreven, T.; Montgomery, J. A., Jr.; Peralta, J. E.; Ogliaro, F.; Bearpark, M.; Heyd, J. J.; Brothers, E.; Kudin, K. N.; Staroverov, V. N.; Keith, T.; Kobayashi, R.; Normand, J.; Raghavachar, K.; Rendell, A.; Burant, J. C.; Iyengar, S. S.; Tomasi, J.; Cossi, M.; Rega, N.; Millam, J. M.; Klene, M.; Knox, J. E.; Cross, J. B.; Bakken, V.; Adamo, C.; Jaramillo, J.; Gomperts, R.; Stratmann, R. E.; Yazyev, O.; Austin, A. J.; Cammi, R.; Pomelli, C.; Ochterski, J. W.; Martin, R. L.; Morokuma, K.; Zakrzewski, V. G.; Voth, G. A.; Salvador, P.; Dannenberg, J. J.; Dapprich, S.; Daniels, A. D.; Farkas, O.; Foresman, J. B.; Ortiz, J. V.; Cioslowski, J.; Fox, D. J. *Gaussian 09, Revision D.01*, Gaussian, Inc.: Wallingford CT, 2010.

27. Zhao, Y.; Truhlar, D. G., Density Functionals With Broad Applicability In Chemistry. *Acc. Chem. Res.* **2008,** *41* (2), 157-167.

28. Zhao, Y.; Truhlar, D. G., The M06 Suite Of Density Functionals For Main Group Thermochemistry, Thermochemical Kinetics, Noncovalent Interactions, Excited States, And Transition Elements: Two New Functionals And Systematic Testing Of Four M06-Class Functionals And 12 Other Functionals. *Theor. Chem. Acc.* **2008,** *120* (1-3), 215-241.

29. Mardirossian, N.; Head-Gordon, M., How Accurate Are the Minnesota Density Functionals for Noncovalent Interactions, Isomerization Energies, Thermochemistry, and Barrier Heights Involving Molecules Composed of Main-Group Elements? *J. Chem. Theory Comput.* **2016**.

30. Tomasi, J.; Mennucci, B.; Cances, E., The IEF Version Of The PCM Solvation Method: An Overview Of A New Method Addressed To Study Molecular Solutes At The QM Ab Initio Level. *J. Mol. Struct. THEOCHEM* **1999,** *464* (1-3), 211-226.

31. Tomasi, J.; Mennucci, B.; Cammi, R., Quantum Mechanical Continuum Solvation Models. *Chem. Rev.* **2005,** *105* (8), 2999-3093.

32. Mennucci, B.; Tomasi, J., Continuum Solvation Models: A New Approach To The Problem Of Solute's Charge Distribution And Cavity Boundaries. *J. Chem. Phys.* **1997,** *106* (12), 5151-5158.

33. Mennucci, B.; Cances, E.; Tomasi, J., Evaluation Of Solvent Effects In Isotropic And Anisotropic Dielectrics And In Ionic Solutions With A Unified Integral Equation Method: Theoretical Bases, Computational Implementation, And Numerical Applications. *J. Phys. Chem. B* **1997,** *101* (49), 10506-10517.

34. Marenich, A. V.; Ho, J.; Coote, M. L.; Cramer, C. J.; Truhlar, D. G., Computational electrochemistry: prediction of liquid-phase reduction potentials. *Phys. Chem. Chem. Phys.* **2014,** *16* (29), 15068-15106.

35. Marenich, A. V.; Cramer, C. J.; Truhlar, D. G., Universal Solvation Model Based on Solute Electron Density and on a Continuum Model of the Solvent Defined by the Bulk Dielectric Constant and Atomic Surface Tensions. *J. Phys. Chem. B* **2009,** *113* (18), 6378-6396.

36. Cances, E.; Mennucci, B.; Tomasi, J., A New Integral Equation Formalism For The Polarizable Continuum Model: Theoretical Background And Applications To Isotropic And Anisotropic Dielectrics. *J. Chem. Phys.* **1997,** *107* (8), 3032-3041.

37. Schuchardt, K. L.; Didier, B. T.; Elsethagen, T.; Sun, L.; Gurumoorthi, V.; Chase, J.; Li, J.; Windus, T. L., Basis Set Exchange: A Community Database for Computational Sciences. *J. Chem. Inf. Model* **2007,** *47* (3), 1045-1052.

38. Feller, D., The Role of Databases in Support of Computational Chemistry Calculations. *J. Comp. Chem.* **1996,** *17* (13), 1571-1586.

39. Zhao, Y.; Truhlar, D. G., Density Functional Calculations of E2 and S(N)2 Reactions: Effects of the Choice of Density Functional, Basis Set, and Self-Consistent Iterations. *J. Chem. Theory Comput.* **2010,** *6* (4), 1104-1108.

40. Bushnell, E. A. C.; Boyd, R. J., Assessment of Several DFT Functionals in Calculation of the Reduction Potentials for Ni–, Pd–, and Pt–Bis-ethylene-1,2-dithiolene and -Diselenolene Complexes. *J. Phys. Chem. A* **2015,** *119* (5), 911-918.

41. Bushnell, E. A. C.; Burns, T. D.; Boyd, R. J., The One-Electron Reduction Of Dithiolate And Diselenolate Ligands. *Phys. Chem. Chem. Phys.* **2014,** *16* (22), 10897-10902.

42. Bushnell, E. A. C.; Burns, T. D.; Boyd, R. J., The One-Electron Oxidation of a Dithiolate Molecule: The Importance of Chemical Intuition. *J. Chem. Phys.* **2014,** *140* (18), 18A519.

43. Cances, E.; Mennucci, B., New applications of integral equations methods for solvation continuum models: ionic solutions and liquid crystals. *J. Math. Chem.* **1998,** *23* (3-4), 309-326.

44. Llano, J.; Eriksson, L. A., First Principles Electrochemistry: Electrons And Protons Reacting As Independent Ions. *J. Chem. Phys.* **2002,** *117* (22), 10193-10206.

45. Lu, T.; Chen, F., Multiwfn: A multifunctional wavefunction analyzer. *J. Comput. Chem.* **2012,** *33* (5), 580-592.

Figure 1 The SOMO and HOMO of the reduced (S/Se-1) and neutral (S/Se0) forms of Ni-bis(dithiolene) and -bis(diselenolene) complexes and hydroxyl radical.

Figure 2 Gibbs reaction energies for the attack of OH to a) S0 and b) S0.

Figure 3 Gibbs reaction energies for the attack of OH to a) S-1 and b) Se-1.

Figure 4 Gibbs reaction energies for the loss of H+ and H• from S0-S and Se0-Se.

Figure 5 Gibbs reaction energies for the loss of H+ and H• from S-1-S and Se-1-Se.

Figure 6 The Gibbs reaction energies for the loss of H+ and H• from S0-C and Se0-C.

Figure 7 The Gibbs reaction energies for the loss of H+ and H• from S-1-C and Se-1-C.

Figure 8 Gibbs reaction energies for the rearrangement between SX-Ni and SX-S and for the loss of H+ and H• from SX-Ni. Where X = 0 or -1.

Figure 9 Gibbs reaction energies for the recovery of the S0 and Se0 catalysts from S0-S and Se0-Se, respectively.

Figure 10 Gibbs reaction energies for the recovery of the S-1 and Se-1 catalysts from S-1-S and Se-1-Se, respectively.

Figure 11 Gibbs reaction energies for the recovery of the S0 and Se0 catalysts from S-1-S and Se-1-Se, respectively.